

# Modeling Diverse Chemical Reactions for Single-step Retrosynthesis via Discrete Latent Variables

Huarui He

CAS Key Laboratory of Technology in GIPAS,  
University of Science and Technology of China,  
Hefei, China  
huaruihe@mail.ustc.edu.cn

Yunfei Liu

CAS Key Laboratory of Technology in GIPAS,  
University of Science and Technology of China,  
Hefei, China  
yf1274540173@mail.ustc.edu.cn

Jie Wang\*

CAS Key Laboratory of Technology in GIPAS,  
University of Science and Technology of China,  
Institute of Artificial Intelligence, Hefei Comprehensive  
National Science Center,  
Hefei, China  
jiawangx@ustc.edu.cn

Feng Wu

CAS Key Laboratory of Technology in GIPAS,  
University of Science and Technology of China,  
Hefei, China  
fengwu@ustc.edu.cn

## ABSTRACT

Single-step retrosynthesis is the cornerstone of retrosynthesis planning, which is a crucial task for computer-aided drug discovery. The goal of single-step retrosynthesis is to identify the possible reactants that lead to the synthesis of the target product in one reaction. By representing organic molecules as canonical strings, existing sequence-based retrosynthetic methods treat the product-to-reactant retrosynthesis as a sequence-to-sequence translation problem. However, most of them struggle to identify diverse chemical reactions for a desired product due to the deterministic inference, which contradicts the fact that many compounds can be synthesized through various reaction types with different sets of reactants.

In this work, we aim to increase reaction diversity and generate various reactants using discrete latent variables. We propose a novel sequence-based approach, namely RetroDCVAE, which incorporates conditional variational autoencoders into single-step retrosynthesis and associates discrete latent variables with the generation process. Specifically, RetroDCVAE uses the Gumbel-Softmax distribution to approximate the categorical distribution over potential reactions and generates multiple sets of reactants with the variational decoder. Experiments demonstrate that RetroDCVAE outperforms state-of-the-art baselines on both benchmark dataset and home-made dataset. Both quantitative and qualitative results show that RetroDCVAE can model the multi-modal distribution over reaction types and produce diverse reactant candidates.

\*Corresponding Author

Permission to make digital or hard copies of all or part of this work for personal or classroom use is granted without fee provided that copies are not made or distributed for profit or commercial advantage and that copies bear this notice and the full citation on the first page. Copyrights for components of this work owned by others than ACM must be honored. Abstracting with credit is permitted. To copy otherwise, or republish, to post on servers or to redistribute to lists, requires prior specific permission and/or a fee. Request permissions from [permissions@acm.org](mailto:permissions@acm.org).

CIKM '22, October 17–22, 2022, Atlanta, GA

© 2022 Association for Computing Machinery.

## CCS CONCEPTS

• **Applied computing** → **Computational biology**; *Chemistry*; • **Computing methodologies** → *Natural language processing*; *Latent variable models*.

## KEYWORDS

Retrosynthesis, Variational Autoencoder, Transformer, Graph Neural Network, Discrete Latent Variable

## ACM Reference Format:

Huarui He, Jie Wang, Yunfei Liu, and Feng Wu. 2022. Modeling Diverse Chemical Reactions for Single-step Retrosynthesis via Discrete Latent Variables. In *Proceedings of Make sure to enter the correct conference title from your rights confirmation email (CIKM '22)*. ACM, New York, NY, USA, 11 pages.

## 1 INTRODUCTION

As a fundamental problem in organic chemistry, retrosynthesis planning refers to the technique to iteratively deconstruct a compound into intermediates or simpler precursors, until a set of commercially available reactants is reached. Since we can solve retrosynthesis planning by searching backwards and recursively applying single-step retrosynthesis to unavailable molecules, this work focuses on single-step retrosynthesis whose goal is to generate a set of reactants that leads to the one-step synthesis of the desired product. In recent years, we have witnessed the great achievement of computer-aided synthesis planning (CASP) [6] in many real-world applications, such as drug design [24], environmental protection [42], as well as materials science [51].

Given that the simplified molecular-input line-entry system (SMILES) [46] can represent arbitrary molecules as strings, researchers formulate the single-step retrosynthesis task as a machine translation problem [22, 41, 53]. Therefore, sequence-based approaches in natural language processing [40, 44] lead to a simple end-to-end formulation that exempts retrosynthesis from reaction templates and domain knowledge. As the extract of high-quality reaction templates requires considerable experience and expertise, the sequence-based retrosynthesis has attracted increasing attention and shown promise as a prevailing template-free approach.

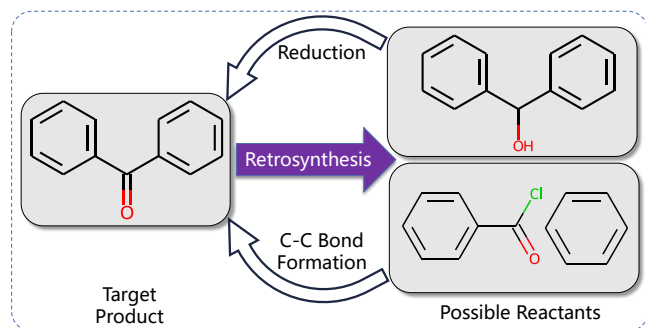


**Figure 1: Illustration of single-step retrosynthesis with two possible reactions. We can synthesize the target product Benzophenone using different sets of reactants through different reactions. Either of the synthesis schemes is feasible. Specifically, Benzophenone (Left) can be synthesized by Benzhydrol through Reduction (Top) or by Benzoyl chloride and Benzene through C-C bond formation (Bottom).**

However, existing work [22, 41, 43, 53] that adapts sequence-to-sequence models to retrosynthesis struggles to model the multi-modal distribution over reaction types. For example, Figure 1 illustrates that Benzophenone can be synthesized in one step by the Reduction reaction or by the C-C bond formation reaction. As existing template-free retrosynthetic models mainly perform deterministic inference, once we finish training and fix the parameters, the retrosynthetic models tend to generate reactants in one direction. That is, existing template-free models may always output only one possible synthesis scheme due to the deterministic inference.

In this paper, we propose a novel template-free model, namely RetroDCVAE, which incorporates stochastic inference into single-step retrosynthesis. Motivated by the fact that a large number of compounds have multiple synthetic schemes, we implicitly model reaction types with categorical latent variables. However, neural networks with discrete latent variables are challenging to train due to the inability to backpropagate through samples. Built upon the Transformer architecture [44], RetroDCVAE incorporates conditional variational autoencoders (CVAE) [36] into the Transformer decoder part and uses the Gumbel-Softmax estimator [15] to support backpropagation of categorical latent variables. To gain insights into the working behaviors of RetroDCVAE, we conduct analysis on a homemade dataset, namely USPTO-DIVERSE, where each target compound owns at least two sets of reactants. Both quantitative and qualitative results show that RetroDCVAE is able to generate diverse reactants for a target product. Furthermore, experiments on the public dataset demonstrate that RetroDCVAE achieves competitive results against state-of-the-art baselines.

The contributions of this work are threefold:

- (1) To the best of our knowledge, we are the first to model the multi-modal distribution in single-step retrosynthesis using discrete CVAE. Moreover, we leverage Gumbel-Softmax [15] to optimize the discrete CVAE for the first time.
- (2) To assess the capacity of modeling the multi-modal distribution over reaction types, we extract all reactions with 1-to-N ( $N \geq 2$ ) products in USPTO-MIT [18] to build a new dataset named USPTO-DIVERSE. That is, each product in USPTO-DIVERSE corresponds to

two or more reactions. We anticipate that USPTO-DIVERSE would exert potential impacts on community.

- (3) We conduct both quantitative and qualitative analysis to show the effectiveness of the proposed RetroDCVAE. Extensive experiments demonstrate that RetroDCVAE outperforms state-of-the-art template-free baselines on the benchmark dataset USPTO-50k and the homemade dataset USPTO-DIVERSE.

## 2 PRELIMINARIES

In this section, we first formulate the single-step retrosynthetic problem and then introduce basic techniques for multi-modal distribution modeling.

### 2.1 Problem Statement

In this part, we define the single-step retrosynthetic task and present the notations throughout this paper.

Let  $\mathcal{M}$  denote the space of all molecules and  $\mathcal{R}$  denote the space of all chemical reaction types. The single-step retrosynthetic model takes a target molecule  $t \in \mathcal{M}$  as input, and predicts a set of precursor source reactants  $\mathcal{S} \subset \mathcal{M}$  leading to synthesizing  $t$ . Therefore, single-step retrosynthesis is the reverse problem of reaction outcome prediction, whose goal is to predict the major product given the set of reactants. Admittedly, single-step retrosynthesis is more challenging than its reverse problem due to the multi-modal distribution over reaction types for a given product. Formally, a single-step retrosynthetic model aims to find a function  $F$  as

$$F(\cdot) : t \rightarrow \{\mathcal{S}_i\}_{i=1}^b,$$

which outputs at most  $b$  sets of reactants. We expect that  $F$  ranks ground truth or plausible reactants as high as possible. The single-step retrosynthetic model can be learned from the collection of chemical reactions  $\mathcal{D}_{\text{train}} = \{\mathcal{S}_i, t_i\}$  in patents granted by United States Patent Office (USPTO).

From a sequence-based perspective, we use SMILES to represent the target product  $t$  as a string. For example, we represent Benzophenone as O=C(C1C=CC=CC=1)C1C=CC=CC=1. Existing sequence-based retrosynthetic models employ the encoder-decoder architecture. The encoder embeds each token of  $t$  into the continuous vector space and drives a sequence of embeddings as  $\mathbf{x} = \{\mathbf{x}_1, \dots, \mathbf{x}_{T_i}\}$  with  $T_i$  representing the length of the input SMILES string. After that, instead of directly performing deterministic inference and decoding  $\mathbf{x}$ , we aim to implicitly model possible reaction types from  $\mathbf{x}$  and then perform stochastic inference. Given  $\mathbf{x}$ , the multi-modal distribution over reaction types is  $P(\mathbf{z}|\mathbf{x})$ . During the inference phase, we sample a possible reaction type  $\mathbf{z} \in \mathcal{R}$  following the distribution  $\mathbf{z} \sim P(\mathbf{z}|\mathbf{x})$ . According to  $\{\mathbf{x}, \mathbf{z}\}$ , the auto-regressive decoder generates a sequence of chemical symbol predictions  $\mathbf{y} = \{y_1, \dots, y_{T_o}\}$  with  $T_o$  representing the length of output tokens. Finally, *beam search* is applied to derive the string representation of reactants. For example, if the sampled  $\mathbf{z} \in \mathcal{R}$  means C-C bond formation reaction, then the retrosynthetic model aims to synthesize Benzophenone through C-C bond formation reaction and would output C1=CC=CC=C1.C1=CC=CC(C(Cl)=O)=C1 as the final prediction, where “.” is the delimiter of two molecules.

## 2.2 Technical Background

CVAE allows us to tackle problems where the input-to-output mapping is one-to-many, while reducing the need to explicitly specify the structure of the output distribution. CVAE [36] aims to model the underlying conditional distribution  $p(y|x)$ , i.e., the distribution over output variable  $y$ , conditioned on the observed variable  $x$ . Given observation  $x$ , the latent variable  $z$  is drawn from the prior distribution  $p(z|x)$ , and the output  $y$  is generated from the distribution  $p(y|x, z)$ . By assuming  $z$  follows multivariate Gaussian distribution with a diagonal co-variance matrix, we have

$$p(y|x) = \int_z p(y|x, z)p(z|x)dz. \quad (1)$$

The typical CVAE consists of a prior network  $p_\theta(z|x)$  parameterized by  $\theta$  and a recognition network  $q_\phi(z|x, y)$  parameterized by  $\phi$ , which are used to approximate the prior distribution  $p(z|x)$  and the posterior distribution  $p(z|x, y)$ , respectively. The evidence lower bound (ELBO) is

$$\begin{aligned} \mathcal{L}_{\text{ELBO}} &= \mathcal{L}_{\text{REC}} - \mathcal{L}_{\text{KL}} \\ &= \mathbb{E}_{q_\phi(z|x, y)} [\log p_\theta(y|x, z)] - D_{\text{KL}}(q_\phi(z|x, y) \| p_\theta(z|x)) \\ &\leq \log p_\theta(y|x), \end{aligned} \quad (2)$$

where  $\mathcal{L}_{\text{REC}}$  is the negative reconstruction error and  $\mathcal{L}_{\text{KL}}$  denotes the Kullback-Leibler (KL) divergence between the posterior and prior. Therefore, to maximize the ELBO w.r.t. parameters  $\theta$  and  $\phi$  will concurrently maximize the likelihood  $p(y|x)$  and minimize the KL divergence.

**Gumbel-Softmax** is a continuous distribution that can approximate categorical samples. We can easily compute parameter gradients of Gumbel-Softmax via the reparameterization trick [21, 28]. Let  $z$  be a categorical variable with class probabilities  $\pi_1, \pi_2, \dots, \pi_k$ . To draw samples  $z$  from a categorical distribution with class probabilities  $\pi$ , Gumbel [11] and Maddison et al. [25] propose the Gumbel-Max trick, i.e.,

$$z = \text{one\_hot}(\arg \max_{i \in [k]} (g_i + \log \pi_i)),$$

where  $[k] = \{1, 2, \dots, k\}$  and samples  $g_1, \dots, g_k$  are drawn i.i.d. according to Gumbel(0, 1). In practice, the Gumbel(0, 1) distribution can be derived using inverse transform sampling by drawing  $u \sim \text{Uniform}(0, 1)$  and computing  $g = -\log(-\log u)$ .

However, the  $\arg \max$  formulation makes it hard to backpropagate through samples. Jang et al. [15] use the softmax function as a continuous and differentiable approximation to  $\arg \max$ , i.e.,

$$z_i = \frac{\exp((\log \pi_i + g_i)/\tau)}{\sum_{j=1}^k \exp((\log \pi_j + g_j)/\tau)}, \quad \text{for } i \in [k].$$

As the softmax temperature  $\tau$  approaches 0, Jang et al. [15] point out that samples from the Gumbel-Softmax distribution become one-hot and the Gumbel-Softmax distribution becomes identical to the categorical distribution  $p(z)$ .

## 3 METHODOLOGY

The proposed discrete conditional stochastic inference mechanism is widely applicable to existing sequence-based models. As shown

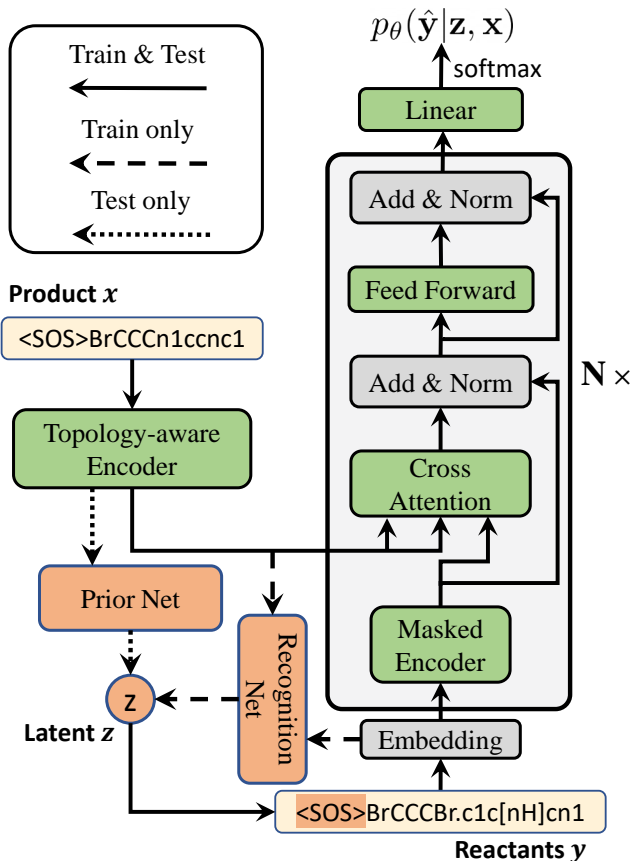


Figure 2: Illustration of proposed RetroDCVAE.

in Figure 2, we follow the encoder-decoder architecture and incorporate the stochastic inference mechanism into the decoder part. As for the encoder part, we perform directed message passing and follow a state-of-the-art template-free baseline [43] to convert the input product SMILES into a sequence of topology-aware embeddings  $x$ . Given  $x$ , we develop a variational auto-regressive decoder to generate the output sequence of chemical symbol predictions  $y$ . In this section, we first briefly introduce the topology-aware encoder in Section 3.1. After that, we elaborate the proposed variational auto-regressive decoder in Section 3.2.

### 3.1 Topology-aware Encoder

We can represent molecules in multiple ways, such as molecular fingerprints [29], SMILES strings [46], and molecular graphs with atoms as nodes and bonds as edges. As Jin et al. [17] criticize that the linear SMILES representation can not well represent the topological context of atoms in a molecular graph, we embed molecules into the continuous vector space as graph embeddings via a topology-aware molecular graph encoder. In the following, we introduce the two critical components of the topology-aware encoder, namely directed message passing neural network (D-MPNN) [48] and topology-aware positional embedding [43].

**3.1.1 D-MPNN.** Unlike atom-oriented message passing in edge-aware MPNNs [13, 26], we follow D-MPNN [48] and use a Directed Graph Convolutional Network (D-GCN) to derive topology-aware atom representations, where message updates are oriented towards directed bonds to prevent totters, or messages being passed back-and-forth between neighbors [48]. Specifically, suppose the message passing performed on an undirected molecular graph  $\mathcal{G}$  with atom features  $x_v$  and bond features  $e_{vw}$  consists of  $T$  steps. On each step  $t$ , hidden states  $h_{vw}^{(t)}$  and messages  $m_{vw}^{(t)}$  associated with each vertex  $v$  are updated through aggregate function  $M^{(t)}$  and update function  $U^{(t)}$  as

$$m_{vw}^{(t+1)} = \sum_{k \in \{N(v) \setminus w\}} M^{(t)}(x_v, x_k, h_{kv}^{(t)}),$$

$$h_{vw}^{(t+1)} = U^{(t)}(h_{vw}^t, m_{vw}^{(t+1)}),$$

where  $N(v)$  is the set of neighboring atoms of  $v$  in the molecular graph  $\mathcal{G}$ . Note that the direction of messages matters since we initialize edge hidden states as  $h_{vw}^{(0)} = \text{ReLU}(W[x_v \| e_{vw}])$  with the trainable matrix  $W$ . After  $T$  iterations, we obtain final atom representations by

$$m_v = \sum_{w \in N(v)} h_{vw}^{(T)},$$

$$h_v = \text{GELU}(W_o[x_v \| m_v]),$$

where  $W_o$  is a trainable matrix, GELU denotes the GELU activation [12], and  $\|$  denotes the concatenation operation.

**3.1.2 Topology-aware token embedding.** To capture atom interactions, the atom representations coming out of D-MPNN are fed into Transformer encoders. Inspired by the relative positional embedding used in Transformer-XL [8], we follow Graph2SMILES [43] and use the topology-aware positional embedding, which is dependent on the shortest path length between atoms in a molecular. Specifically, the attention score between atoms  $v$  and  $w$  in the standard Transformer [44] can be decomposed as

$$\mathbf{A}_{v,w}^{abs} = \mathbf{h}_v^\top \mathbf{W}_q^\top \mathbf{W}_k \mathbf{h}_w + \mathbf{h}_v^\top \mathbf{W}_q^\top \mathbf{W}_k \mathbf{p}_w$$

$$+ \mathbf{p}_v^\top \mathbf{W}_q^\top \mathbf{W}_k \mathbf{h}_w + \mathbf{p}_v^\top \mathbf{W}_q^\top \mathbf{W}_k \mathbf{p}_w,$$

where  $\mathbf{W}_q, \mathbf{W}_k$  are weights for the keys and queries, and  $\mathbf{p}_v, \mathbf{p}_w$  are the absolute positional embeddings corresponding to atoms  $v, w$ . Similar to Transformer-XL [8], we follow Graph2SMILES [43] and reparameterize the four terms as follows,

$$\mathbf{A}_{v,w}^{rel} = (\mathbf{h}_v^\top \mathbf{W}_q^\top + \mathbf{c}^\top) \mathbf{W}_k \mathbf{h}_w + (\mathbf{h}_v^\top \mathbf{W}_q^\top + \mathbf{d}^\top) \mathbf{W}_k \mathbf{r}_{v,w}$$

$$= (\mathbf{h}_v^\top \mathbf{W}_q^\top + \mathbf{c}^\top) \mathbf{W}_k \mathbf{h}_w + (\mathbf{h}_v^\top \mathbf{W}_q^\top + \mathbf{d}^\top) \tilde{\mathbf{r}}_{v,w},$$

where the trainable biases are renamed as  $\mathbf{c}$  and  $\mathbf{d}$  to avoid confusion and  $\mathbf{r}_{v,w}$  is the learnable embedding dependent on the shortest path length between atoms  $v$  and  $w$ . For convenience, we merge  $\mathbf{W}_k \mathbf{r}_{v,w}$  into  $\tilde{\mathbf{r}}_{v,w}$  and use the shortest path length between atoms  $v$  and  $w$  to look up  $\tilde{\mathbf{r}}_{v,w}$  in the trainable positional embedding matrix. Therefore, our encoder integrates topological context into the final token embeddings of the input molecule.

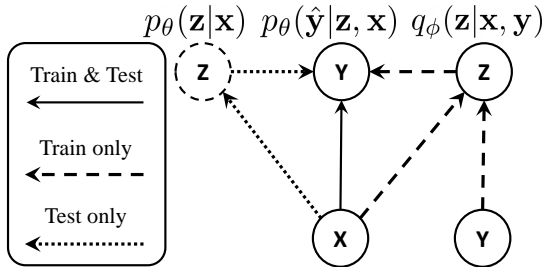


Figure 3: Conditional directed graphical model.

## 3.2 Variational Auto-regressive Decoder

We consider the decoding process as a conditional graphical model concerning three random variables: the encoder output  $\mathbf{x}$ , the discrete latent variable  $\mathbf{z}$ , and the target reactants  $\mathbf{y}$ . Figure 3 illustrates the conditional directed graphical model, where the encoder output is viewed as the observed context. For a given observation  $\mathbf{x}$ , the latent variable  $\mathbf{z}$  is drawn from the prior distribution  $p_\theta(\mathbf{z}|\mathbf{x})$ , and the decoder output  $\hat{\mathbf{y}}$  is generated from the conditional distribution  $p_\theta(\hat{\mathbf{y}}|\mathbf{z}, \mathbf{x})$ . We interpret the one-hot latent variable  $\mathbf{z}$  as the potential reaction type which directs the reactant generating process.

Our variational auto-regressive decoder (VAD) is trained to maximize the conditional log-likelihood  $\log p_\theta(\mathbf{y}|\mathbf{x})$ . As the objective function in Equation 1 is intractable, we use the variational lower bound of the log-likelihood in Equation 2 as a surrogate objective function. Under the reparameterization [21], we can replace an expectation w.r.t.  $q_\phi(\mathbf{z}|\mathbf{x}, \mathbf{y})$  with one w.r.t.  $p(\epsilon)$ . Therefore, we rewrite the ELBO in Equation 2 as

$$\mathcal{L}_{\theta, \phi}(\mathbf{x}, \mathbf{y}) = \mathbb{E}_{p(\epsilon)} [\log p_\theta(\mathbf{y}|\mathbf{x}, \mathbf{z})] - D_{\text{KL}}(q_\phi(\mathbf{z}|\mathbf{x}, \mathbf{y}) \| p_\theta(\mathbf{z}|\mathbf{x})),$$

where  $\mathbf{z} = g_\phi(\mathbf{x}, \mathbf{y}, \epsilon)$ , with  $g_\phi(\cdot, \cdot, \cdot)$  indicating a deterministic, differentiable function and the distribution of the random variable  $\epsilon$  is independent of  $\mathbf{x}$  or  $\mathbf{y}$ . As a result, we can form a simple Monte Carlo estimator  $\tilde{\mathcal{L}}_{\theta, \phi}(\mathbf{x}, \mathbf{y})$  of the ELBO as an empirical lower bound where we use a single noise sample  $\epsilon$  from the Gumbel distribution, i.e.,

$$\epsilon \sim \text{Gumbel}(0, 1),$$

$$\mathbf{z} = g_\phi(\mathbf{x}, \mathbf{y}, \epsilon),$$

$$\tilde{\mathcal{L}}_{\theta, \phi}(\mathbf{x}, \mathbf{y}) = \log p_\theta(\mathbf{y}|\mathbf{x}, \mathbf{z}) - D_{\text{KL}}(q_\phi(\mathbf{z}|\mathbf{x}, \mathbf{y}) \| p_\theta(\mathbf{z}|\mathbf{x})).$$

**Inference process.** Variational inference is a technique for approximating an intractable posterior distribution with a tractable surrogate. Figure 3 illustrates that  $p(\mathbf{z}|\mathbf{x}, \mathbf{y})$  and  $p(\mathbf{z}|\mathbf{x})$  are approximated with a recognition model and a prior model, respectively. Instead of separately and iteratively optimizing the variational parameters per datapoint, we use the same recognition network (with parameters  $\phi$ ) and prior network (with parameters  $\theta$ ) to perform posterior inference over all of the samples  $(\mathbf{x}, \mathbf{y})$  in our dataset. The strategy of sharing variational parameters across datapoints is also known as amortized variational inference [10]. With amortized inference, RetroDCVAE can avoid a per-datapoint optimization loop and leverage the efficiency of stochastic gradient descent.

**Parameter learning.** We summarize the pipeline of variational decoding in Figure 2. Both recognition network  $q_\phi(\mathbf{z}|\mathbf{x}, \mathbf{y})$  and (conditional) prior network  $p_\theta(\mathbf{z}|\mathbf{x})$  are implemented with GRUs [4] as both  $\mathbf{x}$  and  $\mathbf{y}$  are time series data. Taking the prior network  $p_\theta(\mathbf{z}|\mathbf{x})$  for an example, we can formulate the workflow at step  $t$  as

$$\begin{aligned}\mathbf{s}^{(t)} &= \sigma(\mathbf{W}_s \cdot \mathbf{x}^{(t)} + \mathbf{U}_s \cdot \mathbf{h}^{(t-1)} + \mathbf{b}_s), \\ \mathbf{r}^{(t)} &= \sigma(\mathbf{W}_r \cdot \mathbf{x}^{(t)} + \mathbf{U}_r \cdot \mathbf{h}^{(t-1)} + \mathbf{b}_r), \\ \tilde{\mathbf{h}}^{(t)} &= \tanh(\mathbf{W} \cdot \mathbf{x}^{(t)} + \mathbf{U} \cdot (\mathbf{r}^{(t)} \odot \mathbf{h}^{(t-1)}) + \mathbf{b}), \\ \mathbf{h}^{(t)} &= (1 - \mathbf{s}^{(t)}) \odot \mathbf{h}^{(t-1)} + \mathbf{s}^{(t)} \odot \tilde{\mathbf{h}}^{(t)},\end{aligned}$$

where  $\odot$  means the element-wise multiplication. For convenience, we summarize the process as

$$\mathbf{h}^{(t)} = \text{GRU}_\theta(\mathbf{x}^{(t)}, \mathbf{h}^{(t-1)}), \quad \text{for } t \in [T_i],$$

where  $\mathbf{h}^{(0)}$  is initialized to zero vector.

As reaction types are discrete, we employ the Gumbel-Softmax distribution to approximate the latent categorical variable, i.e.,

$$\begin{aligned}\pi_j &= \frac{\exp(\mathbf{h}_j^{(T_i)})}{\sum_{k=1}^K \exp(\mathbf{h}_k^{(T_i)})}, \\ \mathbf{z}_j &= \frac{\exp((\log \pi_j + g_j)/\tau)}{\sum_{k=1}^K \exp((\log \pi_k + g_k)/\tau)}, \quad \text{for } j \in [K],\end{aligned}$$

where  $g_1, \dots, g_K$  are independently drawn from Gumbel(0, 1) and  $K$  is the predefined latent size. Throughout this paper, we further discretize  $\mathbf{z}$  with arg max but use the continuous approximation in the backward pass, which is known as Straight-Through Gumbel Estimator [15]. As depicted in Figure 2, our VAD initializes the *start of the sequence* (namely the “<SOS>” token) based on  $\mathbf{z}$  and then decodes subsequent tokens autoregressively.

## 4 EXPERIMENTAL SETUP

In this section, we detail the experimental setup including datasets, metrics, baselines, and empirical tricks.

### 4.1 Datasets

We empirically evaluate our model on both public and homemade datasets derived from granted patents. We reserve all reactions containing 1-to-N products in USPTO-MIT [18] to create USPTO-DIVERSE, where the maximum  $N$  is 39 in the training set, i.e., there are 39 reactions in the training set that share the same product. In Section 5.1, we provide both quantitative and qualitative results on homemade USPTO-DIVERSE to prove the claim that RetroDCVAE is able to improve the performance of 1-to-N retrosynthesis and generate diverse reactants. In Section 5.2, we compare the proposed approach with existing single-step retrosynthetic methods on the widely used benchmark USPTO-50k [23].

### 4.2 Evaluation Metrics

We mainly use two metrics to evaluate the proposed RetroDCVAE, namely **top- $k$  accuracy** ( $k \in \{1, 3, 5, 10\}$ ) and **coverage**. As the most commonly used metric for retrosynthesis, top- $k$  accuracy is defined as the fraction of correctly predicted reactants with a ranking higher than  $k$ . We count an output sequence as correct only if it matches the ground truth SMILES exactly. Apart from

that, we use the coverage to assess whether RetroDCVAE is able to model the multi-modal distribution. The coverage is defined as the average of the proportion of the correctly predicted ground truth reactions [19]. Therefore, higher coverage indicates that the model is able to generate more accurate and diverse reactant candidates.

### 4.3 Baselines

Following [43], we broadly divide single-step retrosynthetic baselines into two groups according to whether additional features or techniques are used.

**4.3.1 Retrosynthesis with additional features/techniques.** We classify template extraction, atom mapping, and data augmentation into additional features or techniques as each process is computationally expensive. Template-based approaches [3, 7, 30, 39, 47] match the given product with large-scale refined rules or reaction templates and apply them to the product to obtain a set of reactants in single-step retrosynthesis, which has been pointed out to be essentially a symbolic pattern recognition process [32]. Graph-based approaches [3, 33, 35, 37, 39, 45, 47] are built upon atom mapping across chemical reactions, i.e., numbering atoms in a molecular graph to indicate which atom of the reactant(s) becomes which atom of the product(s) [16]. Aug. Transformer [41] and Chemformer [14] explore fully data-driven single-step retrosynthesis by data augmentation, which increases top- $k$  prediction accuracy as well as training costs.

**4.3.2 Retrosynthesis without additional features/techniques.** The proposed RetroDCVAE belongs to this category. This line of research consists of AutoSynRoute [22], SCROP [53], Latent Transformer [2], GET [26], DMP fusion [55], Tied Transformer [19], and Graph2SMILES [43]. All of them treat single-step retrosynthesis as a sequence-to-sequence task and are built upon the Transformer architecture. Note that Graph2SMILES [43] is the closest to RetroDCVAE in implementation, so we treat Graph2SMILES as the base model and compare it with RetroDCVAE on extensive experiments on both public and homemade datasets.

### 4.4 Empirical Methodology

Although CVAE is proved effective in modeling multi-modal distribution [36], Bowman et al. [1] point out that these types of models suffer from *posterior collapse*, i.e.,  $\mathbf{z}$  and  $\mathbf{x}$  become independent if we minimize the KL divergence directly. To alleviate this problem, we use a simple yet effective approach, namely KL annealing [1, 38], where a variable weight is added to the KL term in our objective function during training. Therefore, we aim to maximize the following objective function

$$\tilde{\mathcal{L}}_{\theta, \phi}(\mathbf{x}, \mathbf{y}) = \log p_\theta(\mathbf{y}|\mathbf{x}, \mathbf{z}) - \alpha D_{\text{KL}}(q_\phi(\mathbf{z}|\mathbf{x}, \mathbf{y}) \| p_\theta(\mathbf{z}|\mathbf{x})),$$

where the KL annealing coefficient  $\alpha$  is gradually increased from 0 to 1 over training.

### 4.5 Implementation details

We implement our model using PyTorch and run it on a single NVIDIA GeForce 3090 GPU. Both the encoder and decoder of our model are composed of 6 layers with 8 parallel attention heads. The size of word embedding and atom representation is set to 256. We instantiate the attention sublayers and the position-wise

feed-forward network sublayers with 256 hidden units. Following Graph2SMILES [43], we fix the filter size of Transformer to 2048. We train RetroDCVAE using Adam optimizer [20] with Noam learning rate scheduler [44]. We apply a dropout rate of 0.3 and limit the number of epochs to 2000. The layers of the recognition model and the prior model are both set to 1. We use grid search to find the best latent sizes for different datasets among {10, 20, 30, 60, 120}. Beam search is used to generate the output SMILES during inference with a beam size of 30. To avoid over-tuning, we select the models based on their top-1 accuracy during the validation phase.

## 5 EXPERIMENTAL RESULTS

In this section, we conduct extensive experiments on two datasets to verify the effectiveness of RetroDCVAE. Our experiments are intended to answer the following three research questions.

- **RQ1:** Can RetroDCVAE model the multi-modal distribution over chemical reaction types as claimed?
- **RQ2:** Does the proposed approach achieve competitive results on the benchmark dataset?
- **RQ3:** What role do the discrete latent variables actually play in single-step retrosynthesis?

### 5.1 Evaluation on Homemade Dataset (RQ1)

To assess whether RetroDCVAE can model the multi-modal distribution as claimed, we perform a training/validation/testing split as 8:1:1 over all 1-to-N products in USPTO-MIT [18] to build USPTO-DIVERSE. The product of each reaction in USPTO-DIVERSE corresponds to multiple synthetic schemes, which poses a challenge for deterministic retrosynthetic approaches. We summarize the comparison of Graph2SMILES [43] and RetroDCVAE in Table 1, where the top-1 invalid rate means the proportion of grammatically invalid SMILES in top-1 predictions. By leveraging probabilistic inference, RetroDCVAE significantly reduces the invalid rate and consistently yields improvement in top- $k$  accuracy.

**Table 1: Model performance on USPTO-DIVERSE.**

Model	Top- $k$ accuracy (%)				Top-1 invalid rate (%)
	1	3	5	10	
Graph2SMILES [43]	32.2	45.2	47.9	52.1	8.20
RetroDCVAE	<b>33.4</b>	<b>49.8</b>	<b>54.1</b>	<b>57.1</b>	<b>4.77</b>

We evaluate coverage of top-30 predictions on USPTO-DIVERSE as well. Among 1105 products, 942 have two distinct ground truth reactions, 113 have three distinct ground truth reactions, and 11 have more than five ground truth reactions. Table 2 shows that the RetroDCVAE covers on average 35.8% of the actual reactions contained in the test set, which consistently improves the performance of Graph2SMILES [43].

To examine the quality of retrosynthetic prediction candidates, we compare the proposed RetroDCVAE against Graph2SMILES [43] in terms of top-3 predictions. Figure 4 shows the comparison results. For the same input product, both Graph2SMILES [43] and RetroDCVAE generate grammatically valid reactants. The proposed RetroDCVAE correctly predicts three ground-truth paths,

**Table 2: Coverage evaluation on USPTO-DIVERSE.**

#Reaction per product	#Product	Coverage (%)	
		Graph2SMILES [43]	RetroDCVAE
2	942	33.9	<b>36.6</b>
3	113	30.4	<b>33.6</b>
4	35	23.6	<b>28.6</b>
5	4	<b>10.0</b>	<b>10.0</b>
6	4	8.3	<b>16.7</b>
7	3	<b>23.8</b>	<b>23.8</b>
8	2	6.3	<b>18.9</b>
9	1	11.1	<b>22.2</b>
13	1	7.7	<b>15.4</b>
average		32.9	<b>35.8</b>

while Graph2SMILES [43] generates chemically incorrect reactants and ranks a specious synthetic scheme higher than a correct one. Therefore, the answer to **RQ1** is yes, i.e., RetroDCVAE can alleviate the problem of the multi-modal distribution as claimed.

### 5.2 Evaluation on Public Dataset (RQ2)

Table 3 summarizes the top- $k$  accuracy evaluated on the benchmark dataset USPTO-50k. We divide existing single-step retrosynthetic approaches into two groups. The best top- $k$  accuracy of each group is highlighted with boldface.

Overall, RetroDCVAE achieves competitive results for single-step retrosynthesis and consistently outperforms Graph2SMILES [43] on top- $k$  accuracy. The improvement lies in that RetroDCVAE introduces stochastic inference to structured output prediction, which lowers the risk of over-fitting and reduces the probability of invalid SMILES string output.

Following [43], we divide single-step retrosynthetic methods into two groups according to whether the additional techniques such as templates, atom mapping, and output-side data augmentation are used. Table 3 shows that RetroDCVAE achieves the best top-1 and top-3 accuracies across methods that do not use reaction templates, atom mapping, or output SMILES augmentation. That is, RetroDCVAE achieves state-of-the-art performance while exempting the need of domain knowledge.

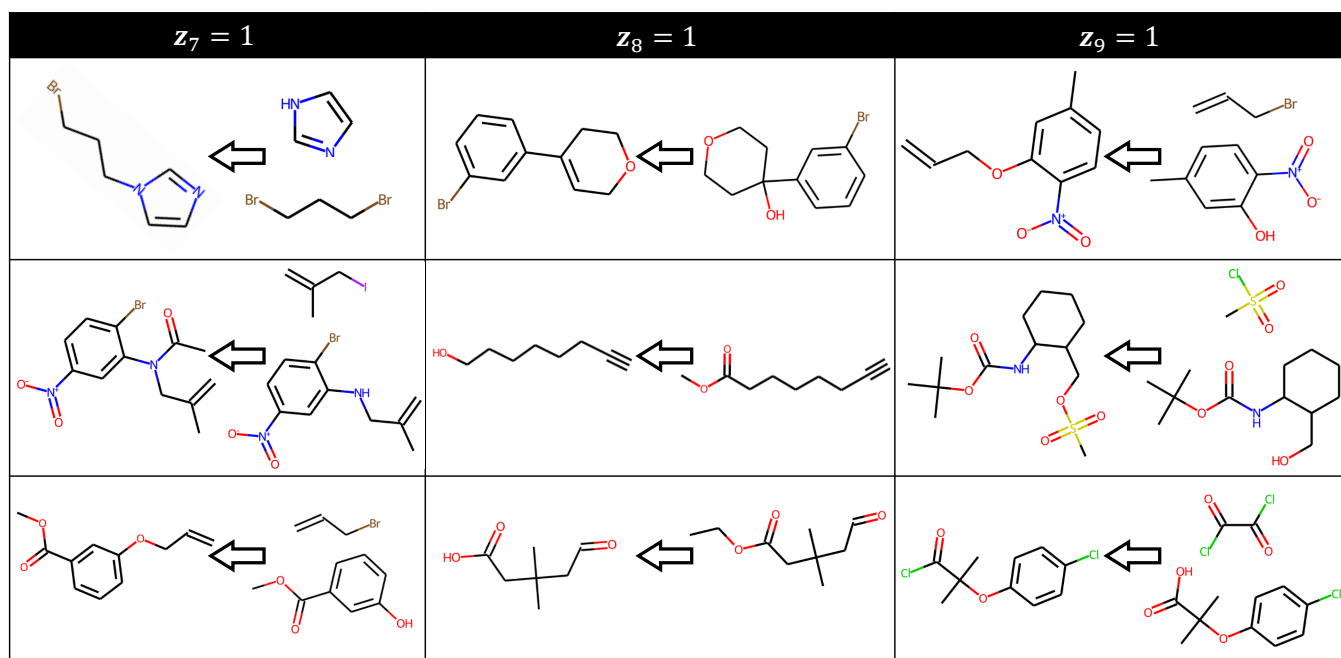
Compared to the second group in Table 3, RetroDCVAE further achieves comparable results against the methods that use additional features or techniques. Specifically, RetroDCVAE even outperforms several template-based baselines [7, 47] in terms of the top-1 accuracy. Therefore, the answer to **RQ2** is yes. We conclude that RetroDCVAE is able to achieve competitive results on the benchmark dataset USPTO-50k.

### 5.3 Further Analysis on Latent Variables (RQ3)

As mentioned in Section 3, we use the Gumbel-Softmax distribution to approximate categorical samples and discretize the latent variable  $z$  with Straight-Through Gumbel Estimator [15]. To gain insights into the working behaviors of RetroDCVAE, we conduct qualitative analysis on the discrete latent variable  $z$  on both public and homemade datasets.

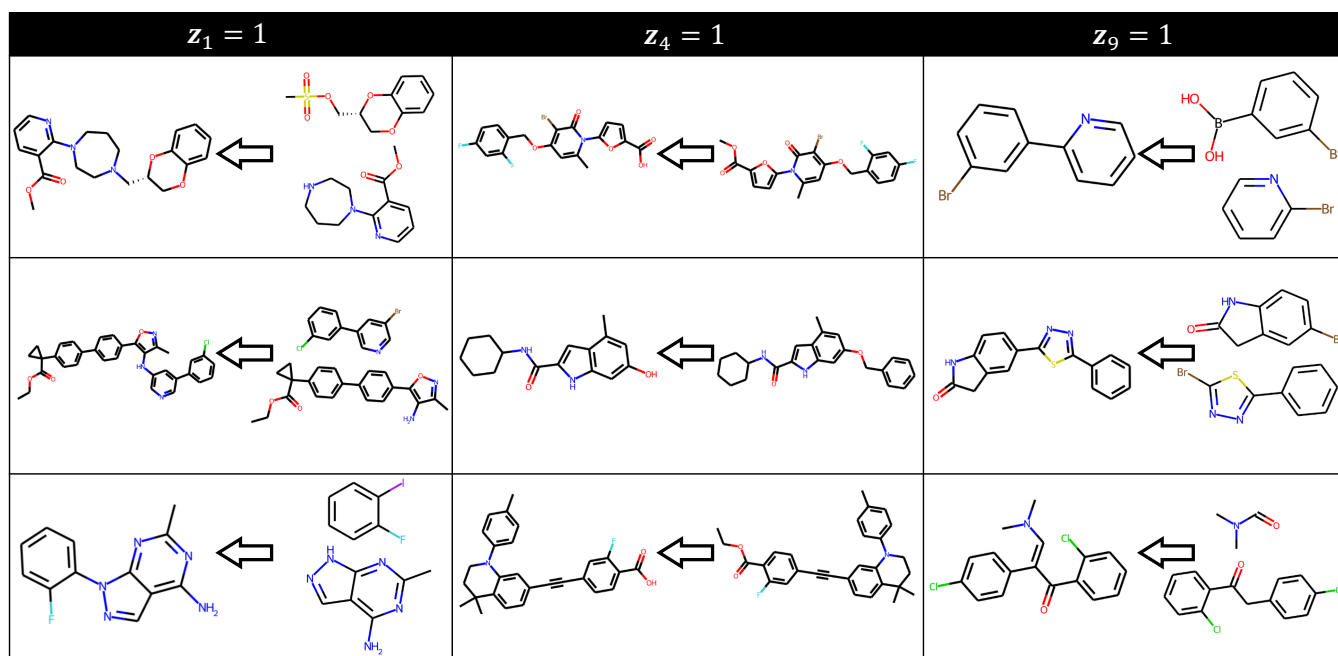
Product		✓ : Correct	✗ : Incorrect
		— : Specious or Plausible Path	
Rank	Ground Truth	Graph2SMILES	RetroDCVAE
1			
2			
3			

Figure 4: Top-3 predictions of Graph2SMILES [43] and RetroDCVAE.

Figure 5: Reactions in USPTO-DIVERSE that corresponding to different  $z$ . As  $z$  is a discrete latent variable,  $z_i = 1$  indicates that  $z$  is the one-hot vector  $e_i$ . RetroDCVAE reads the product SMILES then generates  $z$  and reactants.

**Table 3: Retrosynthesis results on unlabeled USPTO-50k sorted by top-1 accuracy. *Templ.*: reaction templates used; *Map.*: atom-mapping required; *Aug.*: output data augmentation used. Best results for each group of rows are highlighted in bold. The results of previous studies are taken from [43].**

Methods	Top- <i>k</i> accuracy (%)				Techniques used		
	1	3	5	10	<i>Templ.</i>	<i>Map.</i>	<i>Aug.</i>
AutoSynRoute [22]	43.1	64.6	71.8	<b>78.7</b>	✗	✗	✗
SCROP [53]	43.7	60.0	65.2	68.7	✗	✗	✗
Latent Transformer [2]	44.8	64.9	72.4	78.4	✗	✗	✗
GET [26]	44.9	58.8	62.4	65.9	✗	✗	✗
DMP fusion [55]	46.1	65.2	70.4	74.3	✗	✗	✗
Tied Transformer [19]	47.1	67.2	<b>73.5</b>	78.5	✗	✗	✗
Graph2SMILES [43]	52.9	66.5	70.0	72.9	✗	✗	✗
RetroDCVAE ( <i>ours</i> )	<b>53.1</b>	<b>68.1</b>	71.6	74.3	✗	✗	✗
MEGAN [30]	48.1	70.7	78.4	86.1	✗	✓	✗
G2Gs [35]	48.9	67.6	72.5	75.5	✗	✓	✗
RetroXpert [47]	50.4	61.1	62.3	63.4	✓	✓	✓
GTA [33]	51.1	67.6	74.8	81.6	✗	✓	✓
RetroPrime [45]	51.4	70.8	74.0	76.1	✗	✓	✓
GLN [7]	52.5	69.0	75.6	83.7	✓	✓	✗
Aug. Transformer [41]	53.2	-	80.5	85.2	✗	✗	✓
LocalRetro [3]	53.4	<b>77.5</b>	<b>85.9</b>	<b>92.4</b>	✓	✓	✗
GraphRetro [37]	53.7	68.3	72.2	75.5	✗	✓	✗
Chemformer [14]	54.3	-	62.3	63.0	✗	✗	✓
EBM (Dual-TB) [39]	<b>55.2</b>	74.6	80.5	86.9	✓	✓	✓



**Figure 6: Reactions in USPTO-50k that corresponding to different latent variables. Here  $z_i = 1$  indicates that  $z$  is the one-hot vector  $e_i$ . RetroDCVAE reads the product SMILES then generates  $z$  and reactants.**

RetroDCVAE reads an arbitrary product sequence and encodes it using a topology-aware encoder, then the latent variable  $z$  is

sampled according to the product embeddings. Conditioned on  $z$ , RetroDCVAE generates possible reactants using its variational



decoder. To figure out what role the latent variables play, we collect the reactions that associate with the same one-hot vector  $\mathbf{z}$  and present examples in following sections.

**5.3.1 Qualitative Examples on USPTO-DIVERSE.** As depicted in Figure 5, reactions corresponding to the same  $\mathbf{z}$  share many common characteristics. We follow the chemical reaction classification criteria adopted by Schneider et al. [31]. The reactions in the first column can be classified into functional group interconversion (FGI). Moreover, the reactants of the three reactions all contain bromine (Br) atoms. Reactions corresponding to  $\mathbf{z} = \mathbf{e}_8$  in the second column are associated with the formation or disappearance of the C-O bond. In addition, each reaction in the second column only has one reactant. As for the third column, the reactions corresponding to  $\mathbf{z} = \mathbf{e}_9$  can be categorized into functional group addition (FGA).

Therefore, the answer to **RQ3** becomes clear. In general, we can view the discrete latent variables as reaction indicators that guide the generation of distinct reactants. The discrete latent variables reduce grammatically invalid rates and increase reaction diversity for single-step retrosynthesis.

**5.3.2 Qualitative Examples on USPTO-50k.** In addition to the qualitative examples on USPTO-DIVERSE, we analyse the discrete latent variable  $\mathbf{z}$  on the benchmark dataset USPTO-50k [23] as well. Figure 6 presents some reaction examples that correspond to different discrete latent variables. Following the reaction classification criteria in [31], we summarize the reactions in each column as follows.

The reactions corresponding to  $\mathbf{z} = \mathbf{e}_1$  in the first column are associated with the formation of the C-C bond. And the reactions in the second column belong to the deprotection reaction, where a protecting group is modified by converting it into a functional group. Finally, reactions in the third column are all heteroatom alkylation and arylation reactions. Therefore, the conclusion in Section 5.3.1 still holds. The discrete latent variable  $\mathbf{z}$  works as a reaction indicator that guides the generation of distinct sets of reactants. Moreover, the proposed discrete latent variables may have the potential to automatically classify unlabeled reactions in granted patents, reducing the need for experience and expertise.

## 6 DISCUSSION

In this work, we present RetroDCVAE, a novel single-step retrosynthetic approach inspired by CVAE. To delve deeper into the property of RetroDCVAE, we discuss the advantages and limitation of RetroDCVAE in Section 6.1 and Section 6.2, respectively.

### 6.1 Advantages of RetroDCVAE

The proposed RetroDCVAE aims to model the multi-modal distribution over reaction types via discrete latent variables. Compared with state-of-the-art single-step retrosynthetic models [3, 14, 37, 39], RetroDCVAE reduces the need for reaction templates, atom mapping and data augmentation, while maintaining comparable retrosynthetic performance. Compared with existing sequence-based approaches, RetroDCVAE achieves the best top- $k$  accuracy ( $k = 1, 3$ ) for single-step retrosynthesis, while being among the most efficient to train and predict.

Apart from its effectiveness, another significant advantage of RetroDCVAE is its interpretability. Most existing template-free

methods simply output reactant candidates without any explanation. Different from them, RetroDCVAE associates each set of predicted reactants with a discrete latent variable, which we interpret as the corresponding reaction type. The interpretability of RetroDCVAE is expected to have an immediate and strong impact on computer-aided retrosynthetic tasks.

### 6.2 Limitation of RetroDCVAE

One limitation of this work is that RetroDCVAE does not consider catalysts or reagents when generating reactant candidates for the desired product, which is a common fault of existing computer-aided retrosynthetic approaches. In fact, a chemical reaction is related not only to reactants and products, but also to reaction conditions including catalysts, temperature, and reagent concentration. The reaction conditions indicate the difficulty of synthesizing the product to some extent, which is important for retrosynthesis planning. Although it is a pioneer to model reaction types, RetroDCVAE lacks the ability to predict detailed reaction conditions, which can be further improved and extended.

## 7 RELATED WORK

Our work is closely related to single-step retrosynthetic approaches and CVAE based natural language processing (NLP). In this part, we first review single-step retrosynthetic methods in Section 7.1, then briefly introduce CVAE and its variants in Section 7.2.

### 7.1 Single-step Retrosynthesis

An increasing number of machine learning approaches have emerged to assist in designing synthetic schemes for a target product. We broadly categorize them into template-based and template-free.

**7.1.1 Template-based retrosynthesis.** Relying on domain knowledge, template-based methods [3, 5, 7, 32, 39, 47] match the given products with large-scale chemical rules or reaction templates. These rules can be hand-encoded by human experts or automatically extracted from data. This procedure is challenging because encoding which adjacent functional groups influence the outcome of a reaction requires an understanding of the underlying mechanisms. Despite their interpretability, template-based methods are criticized for poor generalization to new and rare reactions [22, 37], which entails a paradigm shift to template-free approaches.

**7.1.2 Template-free retrosynthesis.** According to the leading data format during training, template-free approaches fall into two categories, namely graph edit-based and translation-based. The first category views retrosynthesis as graph transformations. Specifically, [35, 37, 45, 47] first identify reaction centers, then perform graph or sequence recovery. Translation-based methods formulate the product-to-reactant process of single-step retrosynthesis as SMILES-to-SMILES translation, typically with sequence models such as Transformer [9, 22, 41, 49]. Some variants of the second category perform pretraining, rerank the predictions, or leverage graph topology to enhance performance [14, 39, 43, 55].

### 7.2 Conditional Generative Models in NLP

Formulating single-step retrosynthesis as machine translation, we draw inspiration from conditional generative models in NLP. Sohn

et al. [36] propose CVAE to perform probabilistic inference and make diverse predictions, where the Gaussian latent variables are used to model complex structured output representations. Pagnoni et al. [27] introduce CVAE to neural machine translation for conditional text generation, while Zhao et al. [52] and Serban et al. [34] apply continuous latent variables to diverse dialogue generation. In addition, MojiTalk [54] leverages CVAE variants to explicitly control the emotion and sentiment of generated text. Yu et al. [50] propose a multi-pass hierarchical conditional variational autoencoder to improve automatic storytelling. However, the aforementioned methods only consider continuous latent variables, which is unfit for retrosynthesis given the discrete nature of chemical reactions. Unlike them, we use discrete latent variables to guide reactant generation and leverage Gumbel-Softmax approximation to support backpropagation, leading to the novelty of this work.

## 8 CONCLUSION

In this paper, we present RetroDCVAE, a template-free retrosynthesizer that is able to generate diverse reactant candidates via discrete conditional variational autoencoders. Extensive experiments on both public and homemade datasets demonstrate that RetroDCVAE consistently outperforms template-free baselines on single-step retrosynthesis. One limitation of RetroDCVAE is that we do not take into account factors such as catalysts and reagent concentration during the synthetic process, which is a common fault of existing computer-aided retrosynthetic approaches. In future work, we aim to consider detailed reaction conditions and extend RetroDCVAE to multi-step retrosynthesis, i.e., the retrosynthesis planning task. We anticipate that RetroDCVAE would exert potential impacts on modern drug discovery, particularly in accelerating the development of treatments and drugs for COVID-19.

## REFERENCES

- [1] Samuel R. Bowman, Luke Vilnis, Oriol Vinyals, Andrew M. Dai, Rafal Józefowicz, and Samy Bengio. 2016. Generating Sentences from a Continuous Space. In *Proc. of CoNLL*.
- [2] Benson Chen, Tianxiao Shen, Tommi S Jaakkola, and Regina Barzilay. 2019. Learning to make generalizable and diverse predictions for retrosynthesis. *arXiv preprint arXiv:1910.09688* (2019).
- [3] Shuan Chen and Yousung Jung. 2021. Deep Retrosynthetic Reaction Prediction using Local Reactivity and Global Attention. *JACS Au* (2021).
- [4] Kyunghyun Cho, Bart van Merriënboer, Dzmitry Bahdanau, and Yoshua Bengio. 2014. On the Properties of Neural Machine Translation: Encoder-Decoder Approaches. In *Proceedings of SSST@EMNLP 2014*.
- [5] Connor W Coley, Luke Rogers, William H Green, and Klavs F Jensen. 2017. Computer-assisted retrosynthesis based on molecular similarity. *ACS central science* (2017).
- [6] Elias James Corey and W Todd Wipke. 1969. Computer-assisted design of complex organic syntheses. *Science* (1969).
- [7] Hanjun Dai, Chengtao Li, Connor Coley, Bo Dai, and Le Song. 2019. Retrosynthesis Prediction with Conditional Graph Logic Network. In *Proc. of NeurIPS*.
- [8] Zihang Dai, Zhilin Yang, Yiming Yang, Jaime G. Carbonell, Quoc Viet Le, and Ruslan Salakhutdinov. 2019. Transformer-XL: Attentive Language Models beyond a Fixed-Length Context. In *Proc. of ACL*.
- [9] Hongliang Duan, Ling Wang, Chengyun Zhang, Lin Guo, and Jianjun Li. 2020. Retrosynthesis with attention-based NMT model and chemical analysis of “wrong” predictions. *RSC advances* (2020).
- [10] Samuel Gershman and Noah D. Goodman. 2014. Amortized Inference in Probabilistic Reasoning. In *Proc. of CogSci*.
- [11] Emil Julius Gumbel. 1954. *Statistical theory of extreme values and some practical applications: a series of lectures*. US Government Printing Office.
- [12] Dan Hendrycks and Kevin Gimpel. 2016. Bridging Nonlinearities and Stochastic Regularizers with Gaussian Error Linear Units. *arXiv preprint arXiv:1606.08415* (2016).
- [13] Weihua Hu, Bowen Liu, Joseph Gomes, Marinka Zitnik, Percy Liang, Vijay S. Pande, and Jure Leskovec. 2020. Strategies for Pre-training Graph Neural Networks. In *Proc. of ICLR*.
- [14] R. Irwin, S. Dimitriadis, J. He, and E. Bjerrum. 2021. Chemformer: A Pre-Trained Transformer for Computational Chemistry.
- [15] Eric Jang, Shixiang Gu, and Ben Poole. 2017. Categorical Reparameterization with Gumbel-Softmax. In *Proc. of ICLR*.
- [16] Wojciech Jaworski, Sara Szymkuć, Barbara Mikulak-Klucznik, Krzysztof Piecuch, Tomasz Klucznik, Michał Kaźmierowski, Jan Rydzewski, Anna Gambin, Bartosz A Grzybowski, et al. 2019. Automatic mapping of atoms across both simple and complex chemical reactions. *Nat. Comm.* (2019).
- [17] Wengong Jin, Regina Barzilay, and Tommi Jaakkola. 2018. Junction tree variational autoencoder for molecular graph generation. In *Proc. of ICML*.
- [18] Wengong Jin, Connor W. Coley, Regina Barzilay, and Tommi S. Jaakkola. 2017. Predicting Organic Reaction Outcomes with Weisfeiler-Lehman Network. In *Proc. of NeurIPS*.
- [19] Eunji Kim, Dongseon Lee, Youngchun Kwon, Min Sik Park, and Youn-Suk Choi. 2021. Valid, Plausible, and Diverse Retrosynthesis Using Tied Two-Way Transformers with Latent Variables. *J. Chem. Inf. Model.* (2021).
- [20] Diederick P Kingma and Jimmy Ba. 2015. Adam: A method for stochastic optimization. In *Proc. of ICLR*.
- [21] Diederik P. Kingma and Max Welling. 2014. Auto-Encoding Variational Bayes. In *Proc. of ICLR*.
- [22] Kangjie Lin, Youjun Xu, Jianfeng Pei, and Luhua Lai. 2020. Automatic retrosynthetic route planning using template-free models. *Chem. Sci.* (2020).
- [23] Bowen Liu, Bharath Ramsundar, Prasad Kawthekar, Jade Shi, Joseph Gomes, Quang Luu Nguyen, Stephen Ho, Jack Sloane, Paul Wender, and Vijay Pande. 2017. Retrosynthetic reaction prediction using neural sequence-to-sequence models. *ACS central science* (2017).
- [24] Cheng-Hao Liu, Maksym Korablyov, Stanisław Jastrzębski, Paweł Włodarczyk-Pruszyński, Yoshua Bengio, and Marwin HS Segler. 2020. RetroGNN: Approximating Retrosynthesis by Graph Neural Networks for De Novo Drug Design. *arXiv preprint arXiv:2011.13042* (2020).
- [25] Chris J Maddison, Daniel Tarlow, and Tom Minka. 2014. A\* Sampling. In *Proc. of NeurIPS*.
- [26] Kelong Mao, Xi Xiao, Tingyang Xu, Yu Rong, Junzhou Huang, and Peilin Zhao. 2021. Molecular graph enhanced transformer for retrosynthesis prediction. *Neurocomputing* (2021).
- [27] Artidoro Pagnoni, Kevin Liu, and Shangyan Li. 2018. Conditional variational autoencoder for neural machine translation. *arXiv preprint arXiv:1812.04405* (2018).
- [28] Danilo Jimenez Rezende, Shakir Mohamed, and Daan Wierstra. 2014. Stochastic Backpropagation and Approximate Inference in Deep Generative Models. In *Proc. of ICML*.

- [29] David Rogers and Mathew Hahn. 2010. Extended-Connectivity Fingerprints. *J. Chem. Inf. Model.* (2010).
- [30] Mikołaj Sacha, Mikołaj Błaż, Piotr Byrski, Paweł Dąbrowski-Tumański, Mikołaj Chromiński, Rafał Loska, Paweł Włodarczyk-Pruszyński, and Stanisław Jastrzębski. 2021. Molecule Edit Graph Attention Network: Modeling Chemical Reactions as Sequences of Graph Edits. *J. Chem. Inf. Model.* (2021).
- [31] Nadine Schneider, Nikolaus Stiefl, and Gregory A Landrum. 2016. What's what: The (nearly) definitive guide to reaction role assignment. *J. Chem. Inf. Model.* (2016).
- [32] Marwin HS Segler and Mark P Waller. 2017. Neural-symbolic machine learning for retrosynthesis and reaction prediction. *Chemistry—A European Journal* (2017).
- [33] Seung-Woo Seo, You Young Song, June Yong Yang, Seohui Bae, Hankook Lee, Jinwoo Shin, Sung Ju Hwang, and Eunho Yang. 2021. GTA: Graph Truncated Attention for Retrosynthesis. In *Proc. of AAAI*.
- [34] Iulian Vlad Serban, Alessandro Sordani, Ryan Lowe, Laurent Charlin, Joelle Pineau, Aaron C. Courville, and Yoshua Bengio. 2017. A Hierarchical Latent Variable Encoder-Decoder Model for Generating Dialogues. In *Proc. of AAAI*.
- [35] Chence Shi, Minkai Xu, Hongyu Guo, Ming Zhang, and Jian Tang. 2020. A Graph to Graphs Framework for Retrosynthesis Prediction. In *Proc. of ICML*.
- [36] Kihyuk Sohn, Honglak Lee, and Xinchen Yan. 2015. Learning Structured Output Representation using Deep Conditional Generative Models. In *Proc. of NeurIPS*.
- [37] Vignesh Ram Somnath, Charlotte Bunne, Connor W. Coley, Andreas Krause, and Regina Barzilay. 2020. Learning Graph Models for Template-Free Retrosynthesis. *ICML Workshop* (2020).
- [38] Casper Kaae Sønderby, Tapani Raiko, Lars Maaløe, Søren Kaae Sønderby, and Ole Winther. 2016. Ladder Variational Autoencoders. In *Proc. of NeurIPS*.
- [39] Ruoxi Sun, Hanjun Dai, Li Li, Steven Kearnes, and Bo Dai. 2020. Energy-based View of Retrosynthesis. *arXiv preprint arXiv:2007.13437* (2020).
- [40] Ilya Sutskever, Oriol Vinyals, and Quoc V. Le. 2014. Sequence to Sequence Learning with Neural Networks. In *Proc. of NIPS*.
- [41] I.V. Tetko, P. Karpov, and R. Van Deursen. 2020. State-of-the-art augmented NLP transformer models for direct and single-step retro synthesis. *Nat. Comm.* (2020).
- [42] Barry M Trost. 1991. The atom economy—a search for synthetic efficiency. *Science* (1991).
- [43] Zhengkai Tu and Connor W Coley. 2021. Permutation invariant graph-to-sequence model for template-free retrosynthesis and reaction prediction. *arXiv preprint arXiv:2110.09681* (2021).
- [44] Ashish Vaswani, Noam Shazeer, Niki Parmar, Jakob Uszkoreit, Llion Jones, Aidan N Gomez, Lukasz Kaiser, and Illia Polosukhin. 2017. Attention is all you need. In *Proc. of NeurIPS*.
- [45] Xiaorui Wang, Yuquan Li, Jiezhong Qiu, Guangyong Chen, Huanxiang Liu, Benben Liao, Chang-Yu Hsieh, and Xiaojun Yao. 2021. RetroPrime: A Diverse, plausible and Transformer-based method for Single-Step retrosynthesis predictions. *Chemical Engineering Journal* (2021).
- [46] David Weininger. 1988. SMILES, a chemical language and information system. 1. Introduction to methodology and encoding rules. *J. Chem. Inf. Model.* (1988).
- [47] Chaochao Yan, Qianggang Ding, Peilin Zhao, Shuangjia Zheng, Jinyu Yang, Yang Yu, and Junzhou Huang. 2020. RetroXpert: Decompose Retrosynthesis Prediction Like A Chemist. In *Proc. of NeurIPS*.
- [48] Kevin Yang, Kyle Swanson, Wengong Jin, Connor W. Coley, Philipp Eiden, Hua Gao, Angel Guzman-Perez, Timothy Hopper, Brian Kelley, Miriam Mathea, Andrew Palmer, Volker Settels, Tommi S. Jaakkola, Klavs F. Jensen, and Regina Barzilay. 2019. Analyzing Learned Molecular Representations for Property Prediction. *J. Chem. Inf. Model.* (2019).
- [49] Qingyi Yang, Vishnu Sresht, Peter Bolgar, Xinjun Hou, Jacquelyn L Klug-McLeod, Christopher R Butler, et al. 2019. Molecular Transformer unifies reaction prediction and retrosynthesis across pharma chemical space. *Chemical Communications* (2019).
- [50] Meng-Hsuan Yu, Juntao Li, Danyang Liu, Bo Tang, Haisong Zhang, Dongyan Zhao, and Rui Yan. 2020. Draft and Edit: Automatic Storytelling Through Multi-Pass Hierarchical Conditional Variational Autoencoder. In *Proc. of AAAI*.
- [51] Shuai Yuan, Jun-Sheng Qin, Jialuo Li, Lan Huang, Liang Feng, Yu Fang, Christina Lollar, Jiandong Pang, Liangliang Zhang, Di Sun, et al. 2018. Retrosynthesis of multi-component metal-organic frameworks. *Nat. Comm.* (2018).
- [52] Tiancheng Zhao, Ran Zhao, and Maxine Eskénazi. 2017. Learning Discourse-level Diversity for Neural Dialog Models using Conditional Variational Autoencoders. In *Proc. of ACL*.
- [53] Shuangjia Zheng, Jiahua Rao, Zhongyue Zhang, Jun Xu, and Yuedong Yang. 2020. Predicting Retrosynthetic Reactions Using Self-Corrected Transformer Neural Networks. *J. Chem. Inf. Model.* (2020).
- [54] Xianda Zhou and William Yang Wang. 2018. MojiTalk: Generating Emotional Responses at Scale. In *Proc. of ACL*.
- [55] Jinhua Zhu, Yingce Xia, Tao Qin, Wengang Zhou, Houqiang Li, and Tie-Yan Liu. 2021. Dual-view Molecule Pre-training. *arXiv preprint arXiv:2106.10234* (2021).